Modeling of Ground Excavation with the Particle Finite-Element Method

Josep Maria Carbonell[1]; Eugenio Oñate[2]; and Benjamín Suárez[3]

Abstract: An excavation process is a nonlinear dynamic problem that includes geometrical, material, and contact nonlinearities. The simulation of ground excavation has to face contact interaction in a changing geometry composed by several solid domains. The particle finite-element method (PFEM) is based on a Lagrangian description for modeling the motion of a continuum medium. The PFEM is particularly suitable for modeling a fluid motion with free surfaces. The application of the PFEM in ground excavation includes the use of the remeshing process, α-shape concepts for detecting the domain boundary, contact mechanics laws, material constitutive models, and surface wear models. Everything is correctly matched to quantify the excavation and the corresponding damage caused to the ground. The erosion and wear parameters of the soil/rock material govern the evolution of the excavation process. The preliminary results presented in this paper show that the PFEM it is a very suitable tool for the simulation of ground excavation processes.

DOI: 10.1061/(ASCE)EM.1943-7889.0000086

CE Database subject headings: Particles; Finite element method; Excavation; Geometry.

Author keywords: Particle finite-element method; Contact mechanics; Wear.

Introduction

The objective of this work is to describe a new procedure for simulating excavation processes. An excavation is a complex problem that involves large deformations and displacements and multiple contacts between solid domains. The solid domains are composed by the continuum media that represent geomaterials and the cutting tools.

Material responses are governed by their specific constitutive equations but the rules for the excavation and for the wear of the ground surface are not the same. The excavation is controlled by parameters that have not a direct influence on the constitutive response. Some materials are easily penetrable and disgregable, others have a high superficial hardness or a high level of abrassivity. These properties vary from material to material and influence the excavability of a terrain.

Previous attempts to model numerically ground excavation processes have been made with the discrete element method (DEM) (Labra et al. 2008). The difficulties of the DEM include the modeling of the complex tool-soil/rock interactions with adequate constitutive models for representing the evolution of the material properties of the different interacting continua during the excavation process. Most of these difficulties are overcome with the particle finite-element method (PFEM) presented in this work.

The overall difficulty is to model a problem that has rapid dynamical changes in a system full of nonlinearities including geometrical, material, and frictional contact nonlinearities. The PFEM used in this work is very suitable for treating large material deformations and rapidly changing boundaries, which are typical of excavation processes.

PFEM has its foundation on the Lagrangian description of the motion of a continuum medium built from a set of particles with known physical properties. The finite-element method is used to solve the continuum equations in the global domain.

The origins of the PFEM can be found in computational fluid dynamics problems (Idelsohn et al. 2003; Oñate et al. 2004). Current research is focused in applications of PFEM in several problems that go beyond the fluid motion description (Idelsohn et al. 2004; Oñate et al. 2006, 2008). Fluid-structure interaction problems with rigid bodies, erosion processes (bed erosion, unsteady flows), mixing processes, coupled thermoviscous problems, and thermal diffusion are some of the applications of the PFEM. A first application of the PFEM in solid mechanics can be found in (Oliver et al. 2007). This work is the first application of the PFEM for the simulation of ground excavation.

Basis of the PFEM for Continuum Mechanics

In the PFEM, the continuum is described as a cloud of particles of infinitesimal size. The particles contain all the properties of the continuum medium (displacements, velocities, strains, stresses, material properties, internal variables, etc.). This cloud of particles is the basis of the PFEM. From the cloud a finite-element mesh is generated at each time step using a Delaunay triangulation (Calvo et al. 2003). The properties from the particles are

[1]Ingeniero de Caminos, Canales y Puertos, International Center for Numerical Methods in Engineering (CIMNE), Universitat Politècnica de Catalunya (UPC), Campus Nord, Gran Capitán, s/n, 08034 Barcelona, Spain (corresponding author). E-mail: cpuigbo@cimne.upc.edu

[2]Director, International Center for Numerical Methods in Engineering (CIMNE), Universitat Politècnica de Catalunya (UPC), Campus Nord, Gran Capitán, s/n, 08034 Barcelona, Spain. E-mail: onate@cimne.upc.edu

[3]Head Manager, Dept. de Resistència de Materials i Estructures a l'Enginyeria, Escola Tècnica Superior d'Enginers de Camins Canals i Ports, Universitat Politècnica de Catalunya (UPC), Campus Nord, Jordi Girona, 1-3, 08034 Barcelona, Spain. E-mail: benjamin.suarez@upc.edu

Note. This manuscript was submitted on July 28, 2008; approved on September 2, 2009; published online on September 3, 2009. Discussion period open until September 1, 2010; separate discussions must be submitted for individual papers. This paper is part of the ***Journal of Engineering Mechanics***, Vol. 136, No. 4, April 1, 2010. ©ASCE, ISSN 0733-9399/2010/4-455–463/$25.00.

transferred to the elements of the mesh for the computation. An α-shape technique (Edelsbrunner and Mücke 1994) is used to define the boundaries of the domain and to detect the geometrical contacts at each time step. The motion is described using an updated Lagrangian (UL) formulation (Belytschko et al. 2000). The update of the analysis domain, the boundary recognition, and the treatment of contact between interacting domains via mesh generation are the key features of the PFEM.

Updated Lagrangian Formulation for Description

The basis of the PFEM in this work lie in the equations of standard solid mechanics theory (Bathe 1982; Belytschko et al. 2000). The main dependent variables are the initial density ρ_0, the displacement $\mathbf{u}$, and the Lagrangian measures of stress $\boldsymbol{\sigma}$ and strain $\mathbf{e}$. They depend on the particle position $\mathbf{X}$ and time t. The relevant equations are:

- Mass conservation (continuity equation)

$$\rho(\mathbf{X},t)J(\mathbf{X},t) = \rho_0(\mathbf{X},t) \tag{1}$$

  where ρ=density and J=determinant of the deformation gradient tensor.
- Conservation of linear momentum

$$\frac{\partial \boldsymbol{\sigma}}{\partial \mathbf{X}} + \rho\mathbf{b} = \rho\ddot{\mathbf{u}} \tag{2}$$

  where $\mathbf{b}$=force for unit of mass; $\ddot{\mathbf{u}}$=accelerations; and $\boldsymbol{\sigma}$=Cauchy stress tensor.
- Conservation of angular momentum

$$\boldsymbol{\sigma} = \boldsymbol{\sigma}^T \tag{3}$$

- Constitutive equation

In our work, we use a standard damage constitutive model (Oliver et al. 1990)

$$\boldsymbol{\sigma} = (1-d)\mathbf{C}\mathbf{e} \tag{4}$$

where $\mathbf{e}$=linear part of the Green-Lagrange strain tensor; d=damage variable; and $\mathbf{C}$=elastic constitutive tensor.

The integral form of the equilibrium equation is represented by the virtual work principle (PVW). Substituting the finite-element interpolation into the PVW leads to the standard residual equation in the matrix form

$$\mathbf{r} := \mathbf{M}\ddot{\mathbf{u}}^{n+1} - \mathbf{f}^{\text{ext}} + \mathbf{f}^{\text{int}} = 0 \tag{5}$$

where $\mathbf{r}$=residual force vector; $\mathbf{M}$=mass matrix; $\mathbf{f}^{\text{ext}}$=external forces; $\mathbf{f}^{\text{int}}$=internal forces; and $\ddot{\mathbf{u}}^{n+1}$=acceleration for the time step $n+1$.

The solution of above set of equations in time using an UL formulation requires the definition of the boundary and the initial conditions for $\mathbf{u}_0, \dot{\mathbf{u}}_0, \ddot{\mathbf{u}}_0$ and the external forces. Contact forces have a special treatment in the PFEM. They are not considered as external forces. Instead contact is produced by a part of the domain involving contact elements with no mass but with stiffness that follows a particular contact law. That is, $\mathbf{f}^{\text{int}} = \hat{\mathbf{f}}^{\text{int}} + \hat{\mathbf{f}}^{\text{cont}}$ where $\hat{\mathbf{f}}^{\text{cont}}$ denotes the contact forces.

In the UL formulation, every time step has the reference boundary conditions of the previous one. The computation of the internal and contact forces $\hat{\mathbf{f}}^{\text{int}}$ and $\hat{\mathbf{f}}^{\text{cont}}$, as well as the system matrices, are based on the updating of displacements and stresses

$$\mathbf{u}^{t+\Delta t} = \mathbf{u}^t + \Delta\mathbf{u} \tag{6}$$

$$\mathbf{S}^{t+\Delta t} = \boldsymbol{\sigma}^t + \Delta\mathbf{S} \tag{7}$$

where $\mathbf{S}$=second Piola-Kirchhoff stress tensor and $\boldsymbol{\sigma}$=Cauchy stress tensor. Note that $\mathbf{S}^t = \boldsymbol{\sigma}^t$.

All incremental variables are computed at the nodes and the integration points are stored in the particles. Usually, these particles coincide with mesh nodes. There is no reference to the origin of the computations.

For solving the main system of equations [Eq. (5)], an implicit integration scheme is chosen. The system is linearized using the standard Newton-Raphson method and solved in time with the Newmark β scheme (Belytschko et al. 2000). The momentum equation at time step $n+1$ can be written as

$$0 = \mathbf{r}(\mathbf{u}^{n+1}, t^{n+1}) = \mathbf{M}\ddot{\mathbf{u}}^{\mathbf{n+1}} - \mathbf{f}^{\text{ext}}(\mathbf{u}^{n+1}, t^{n+1}) + \mathbf{f}^{\text{int}}(\mathbf{u}^{n+1}, t^{n+1}) \tag{8}$$

The linealization of this nonlinear equation yields the following iterative integration scheme

$$\left(\frac{\mathbf{M}}{\beta\Delta t^2} + \mathbf{K}^{\text{mat}} + \mathbf{K}^{\text{geo}}\right)\Delta\mathbf{u} = \mathbf{f}^{\text{int}} - \mathbf{f}^{\text{ext}} \tag{9}$$

where $\mathbf{K}^{\text{mat}}$=stiffness matrix; $\mathbf{K}^{\text{geo}}$=geometric stiffness matrix; and β=parameter of the Newmark β scheme used to discretize the equations in time. The displacements for the iteration $\nu+1$ are computed as

$$(\mathbf{u}^{n+1})^{\nu+1} = (\mathbf{u}^{n+1})^{\nu} + \Delta\mathbf{u} \tag{10}$$

where $\Delta\mathbf{u}$ is computed by Eq. (9).

Details of the matrices and vectors in Eq. (9) can be found in the classical theory for nonlinear finite-element analysis of continua (Bathe 1982; Belytschko et al. 2000). An important aspect of the integration method is the conservation of energy. Equations have to be able to represent an ideal dynamic process without any win or loss of energy. Newmark integration is undamped for the selected values of its parameters (see Bathe 1982). Even so, it has the tendency for high frequency noise to persist in the solution. By using the Bossack or Hilbert α *methods* (Kuhl and Crisfield 1999), numerical dissipation for high frequencies is improved without degrading the accuracy so much.

Importance of a Particle-Based Method

The PFEM is based on particles for one important reason. After getting the solution for one time step, a new mesh is created and the element information is destroyed. That means that particles must store the information and be the variables container. A particle is different from a node because it is not only a geometric position. It contains all the information about the key variables in the domain and also has the functionality of a node.

In the following we will use the name "particle" or "node" indistinctly. Finite elements find the equilibrium of the continuum equations at the integration points. Some variables like stresses are discontinuous from element to element. When the *Gauss* point information is transferred back to the nodes, the domain does not recover the original state. The transfer of variables between Gauss points to nodes typically leads to a smoothing of the information.

To minimize the error due to the information transfer, only the incremental part of the information is transferred to the nodes (particles). The increment of a variable at a time step is the only error that will be carried out along the analysis. The previous information remains on the particle and is updated at each time step. This is the natural form of the incremental equations in the UL formulation but translated to a particle-based technique. The updating scheme is the following:

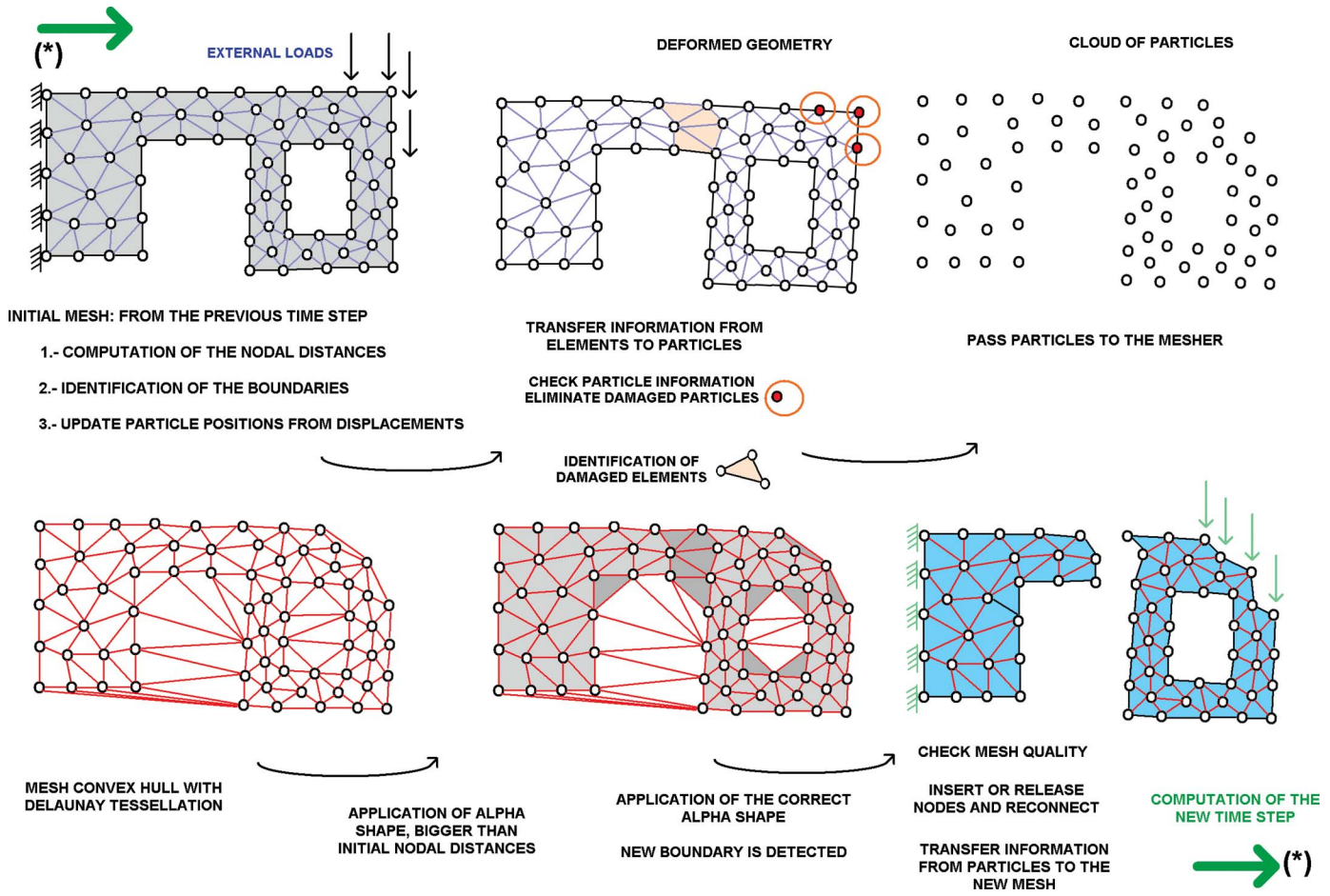

Fig. 1. Use of the remeshing in the PFEM

1. Transfer the stresses from particles to elements

$$\boldsymbol{\sigma}_{\text{particle}}(\rightarrow \boldsymbol{\sigma}_{\text{node}}) \rightarrow \boldsymbol{\sigma}_{\text{integration point}}$$

where the arrow means the transferred variable. Each transfer implies a smoothing operation using the total value of the stresses.

2. Calculate the new stresses

$$\boldsymbol{\sigma}^{t+\Delta t}_{\text{integration point}}$$

3. Calculate the stress increment

$$\boldsymbol{\sigma}^{t+\Delta t}_{\text{integration point}} = \boldsymbol{\sigma}^{t}_{\text{integration point}} + \Delta\boldsymbol{\sigma}_{\text{integration point}} \quad (11)$$

4. Transfer the stress increment to the nodes

$$\Delta\boldsymbol{\sigma}_{\text{integration point}} \rightarrow \Delta\boldsymbol{\sigma}_{\text{particle}}$$

This is the second smoothing involving only the stress increment.

5. Add the nodal stress increment to the historical stress values at the nodes

$$\boldsymbol{\sigma}^{t+\Delta t}_{\text{particle}} = \boldsymbol{\sigma}^{t}_{\text{particle}} + \Delta\sigma_{\text{particle}} \quad (12)$$

This process leads to a minimum smoothing of the stress field.

The accumulated error in the scheme is only due to the smoothing of the stress increment. This is the only part that is carried forward along the analysis steps and it is too small to affect the results.

Remeshing and Boundary Recognition

The PFEM includes the remeshing of the domain as an important step in the analysis. By means of the remeshing, the boundary of the different body entities is identified.

In an excavation process, the geometry of the problem is changing continuously. Geomaterials are excavated and the cutting tools are worn. The geometry of the excavation domain and the tools change at the time these phenomena occurs.

The remeshing of the global domain is also essential for the identification of contact between domains. The particles carry forward enough information to allow the analysis in the new mesh at each time step.

When a result is computed an update of the position is done. Nodes (i.e., the particles) have a new relative position in the space. Delaunay tessellation (Calvo et al. 2003) is used to create a mesh from a cloud of particles in space. This mesh is generated in the new analysis domain at each time step (see Fig. 1).

Through the α-shape technique, the boundary of the bodies is detected and rebuilt. The α-shape method also provides a criteria to accept or throw away new generated triangular elements. Alpha shapes in two dimensions (2D) are related to the Delaunay circumcircles obtained from a Delaunay triangulation. In three-dimensional (3D) problems, the α shapes are related to Delaunay circumspheres. Each particle has a characteristic parameter defined by the mesh size that is compared with the radius of the Delaunay sphere that includes the particle (Fig. 1). This method allows the boundaries to be detected.

J. Eng. Mech., 2010, 136(4): 455-463

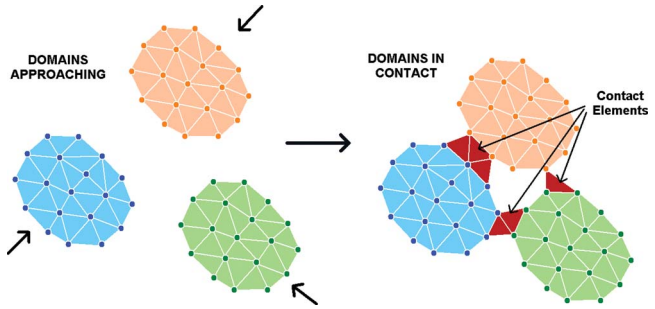

Fig. 2. Alpha-shape detects domains and contact elements when they are close enough

Contact is detected when the two domains are so close as to generate contact elements between the interacting subdomain (Fig. 2). An interface mesh is created anticipating the spatial contact. Hence, a mesh for the domain and a mesh for the interface are generated. This permits to anticipate the collision of the different subdomains.

Treatment of Contact with the PFEM

Detecting the contact is easy with the PFEM. The interaction between bodies is modeled with a thin mesh interface. This interface generates large interacting forces due to the interchange of dynamic energy in the contact region.

Either the penalty method or the Lagrange multipliers method can be used to treat the interaction between the deformable bodies in contact (Wriggers 2006). These two methods have the advantage that the detection of the contact regions is performed in an easy manner via the α-shape technique. The size of the system remains the same when a penalty method is used, i.e., there are not additional degrees of freedom in the system. Even so, the characterization of the penalty parameters and the convergence of the numerical solution are two difficulties that remain and preclude obtaining a good result.

Contact implies compressive and friction forces between the interacting domains. The magnitude of these forces is large for moderate time steps. Big values for the contact forces change the condition of the numerical system adversely and push the analysis toward using small time steps. This jeopardizes the advantages of using an implicit integration scheme.

These problems can be overcome by treating the contact interface as a part of the continuum via the contact element (Fig. 3).

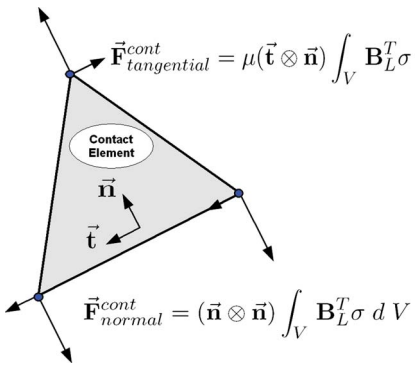

Fig. 3. Contact forces in a contact element

We note that elements lying in the contact interface are not used to define a spring or to assign a direct correspondence in the relative movement of the contact domains. These elements are in fact considered as finite elements with special contact properties.

The first step is to simplify the displacement of the nodes in the contact elements only in the direction of the normal to the contact faces as

$$(\vec{\mathbf{u}}_{cn} \cdot \vec{\mathbf{n}}) > 0 \rightarrow \vec{\mathbf{u}}_{cn} = (\vec{\mathbf{u}}_{cn} \cdot \vec{\mathbf{n}}) \cdot \vec{\mathbf{n}} \tag{13}$$

where $\vec{\mathbf{u}}_{cn}$=displacement in the contact node and $\vec{\mathbf{n}}$=normal to the contact faces at the contact node. For clarity purposes, in the rest of equations, an arrow ($\vec{\cdot}$) is used to identify the variables which are vectors.

The constitutive law in contact elements is a combination of the properties of the interacting domains governed by a special volumetric function. For example, the *Young's* modulus in a contact element is defined as

$$E_{\text{contact element}} = \frac{1}{n} \sum_{\text{node}=1}^{n} E_{\text{node}} \cdot |\boldsymbol{\varepsilon}_{\text{active gap}}|^3 \tag{14}$$

where n=number of nodes per element and $\boldsymbol{\varepsilon}_{\text{active gap}}$=total volumetric deformation of the active contact elements.

The average Young's modulus is multiplied by a cubic function to smooth the transition. The activation of this function depends on the gap. The gap function G_{gap} is a normalized function that takes the normal distance into account between contact faces $D_{\text{face to face}}$ as well as the mesh characteristics h_{node}.

$$G_{\text{gap}} = 1 - \frac{D_{\text{face to face}}}{\frac{1}{n}\left(\sum_{\text{node}=1}^{n} h_{\text{node}}\right)} \tag{15}$$

$$\begin{cases} G_{\text{gap}} \in (-\infty, 0) \Rightarrow G_{\text{gap}} = 0 \\ G_{\text{gap}} \in [0, 1] \end{cases} \tag{16}$$

where distance h_{node}=nodal parameter used in the α-shape detection. Usually, it is the maximum or the average distance of one particle to their neighbor particles (Edelsbrunner and Mücke 1994).

The variable $\boldsymbol{\varepsilon}_{\text{active gap}}$ is updated while the contact nodes belong to an active element. The total volumetric strain must be negative to take it into account

$$\boldsymbol{\varepsilon}_{\text{active gap}} \in (0, +\infty) \Rightarrow \boldsymbol{\varepsilon}_{\text{active gap}} = 0 \tag{17}$$

when $\boldsymbol{\varepsilon}_{\text{active gap}}$=0 contact is not active, and when $\boldsymbol{\varepsilon}_{\text{active gap}}$=−1 the domains undergo fully interaction.

This methodology can be viewed as a nonlinear constitutive law for contact elements. The tangential constitutive tensor is the elastic tensor for a volumetric deformation with a nonlinear Young's modulus. It also introduces certain modifications in the elemental system to improve convergence.

When this contact scheme is applied, the stresses in the contact elements only have a nonzero value in the normal direction to the faces in contact. The resultant forces are projected into the normal direction and only appear when the interacting domains are compressing each other. They can be expressed as follows:

$$(\vec{\mathbf{F}}^{\text{int}}_{cn} \cdot \vec{\mathbf{n}}) > 0 \rightarrow \vec{\mathbf{F}}^{\text{int}}_{cn} = (\vec{\mathbf{F}}^{\text{int}}_{cn} \cdot \vec{\mathbf{n}}) \cdot \vec{\mathbf{n}} \tag{18}$$

The resultant normal forces are typically quite large. The transformation of the elemental forces is performed in the elemental system matrix. This softens the influence in the condition number of the equation system and improves the convergence of the it-

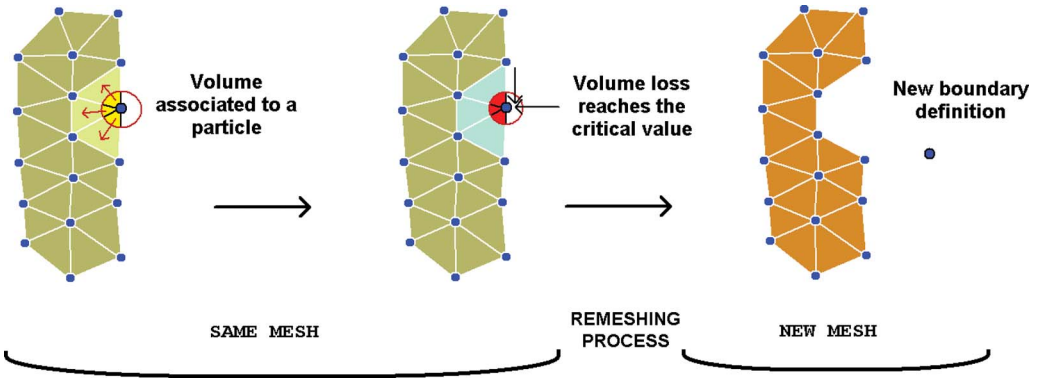

Fig. 4. Removing material and boundary update

erative process. Then a new tangent stiffness matrix appears in the left hand side of the system as

$$\mathbf{K}_{ce}\vec{\mathbf{u}}_{ce} = \vec{\mathbf{F}}^{\text{int}}_{ce} \Rightarrow (\vec{\mathbf{F}}^{\text{int}}_{ce} \cdot \vec{\mathbf{n}}) \cdot \vec{\mathbf{n}} = (\vec{\mathbf{n}} \otimes \vec{\mathbf{n}})\vec{\mathbf{F}}^{\text{int}}_{ce} \tag{19}$$

$$(\vec{\mathbf{n}} \otimes \vec{\mathbf{n}})\mathbf{K}_{ce}(\vec{\mathbf{n}} \otimes \vec{\mathbf{n}})\vec{\mathbf{u}} = (\vec{\mathbf{n}} \otimes \vec{\mathbf{n}})\vec{\mathbf{F}}^{\text{int}}_{ce} \tag{20}$$

where $\mathbf{K}_{ce}$ and $\vec{\mathbf{F}}^{\text{int}}_{ce}$=stiffness matrix and the internal force vector for a contact element, respectively, and $\vec{\mathbf{n}}$=normal to the contact face associated to each node in the contact element. The preceding transformation maintains the symmetry in the elemental stiffness matrices for the contact elements.

Frictional Effects in the Contact Region

Frictional effects are essential to model excavation processes. Friction forces between surfaces are included initially as external forces. The friction process is described by a Coulomb law in the element interface. The tangential external force appears at the contact surface and is proportional to the normal contact force

$$(\vec{\mathbf{F}}^{\text{int}}_{\text{normal}} \cdot \vec{\mathbf{n}}) > 0 \rightarrow \vec{\mathbf{F}}^{\text{frict}}_{\text{tangencial}} = -\mu(\vec{\mathbf{F}}^{\text{int}}_{\text{normal}} \cdot \vec{\mathbf{n}}) \cdot \vec{\mathbf{t}} \tag{21}$$

where $\vec{\mathbf{n}}$ and $\vec{\mathbf{t}}$=normal and the tangential directions to the contact face associated to each node in the contact element (Fig. 3).

Friction resistance to the movement depends on the relative sliding velocity. A body that starts the movement has more friction resistance than other that is already in motion. The relative sliding velocity between the contacting bodies $\dot{\vec{\mathbf{u}}}_t$ is a relevant physical variable that is incorporated to the friction law, as

$$\mu(\dot{\vec{\mathbf{u}}}_t) = \mu_D + (\mu_S - \mu_D)e^{-c\|\dot{\vec{\mathbf{u}}}_t\|} \tag{22}$$

where μ_D and μ_S=dynamic and static friction coefficients, respectively. The constitutive parameter c describes how fast the static coefficient approaches the dynamic one.

To obtain a smooth transition from stick to slip condition, a square root regularization of the Coulomb law is introduced as

$$\vec{\mathbf{F}}^{\text{frict}}_{\text{tangencial}} = -\mu\varphi(\dot{\vec{\mathbf{u}}}_t)\vec{\mathbf{F}}^{\text{int}}_{\text{normal}} \tag{23}$$

where

$$\varphi = \frac{\|\dot{\vec{\mathbf{u}}}_t\|}{\sqrt{\|\dot{\vec{\mathbf{u}}}\|_t^2 + \varepsilon^2}} \tag{24}$$

and the scalar parameter ε denotes the regularization variable, which for $\varepsilon \rightarrow 0$ yields the classical Coulomb law.

To improve the convergence of the system, the elemental stiffness matrix is modified as was done for the normal contact interaction. Then the frictional force is introduced as an internal force and has its correspondence in the left hand side of the equation as

$$\mathbf{K}_{ce}\vec{\mathbf{u}}_{ce} = \vec{\mathbf{F}}^{\text{int}}_{ce} \Rightarrow (\vec{\mathbf{F}}^{\text{int}}_{ce} \cdot \vec{\mathbf{n}}) \cdot \vec{\mathbf{t}} = (\vec{\mathbf{t}} \otimes \vec{\mathbf{n}})\vec{\mathbf{F}}^{\text{int}}_{ce} \tag{25}$$

$$(\vec{\mathbf{t}} \otimes \vec{\mathbf{n}})\mathbf{K}_{ce}(\vec{\mathbf{n}} \otimes \vec{\mathbf{n}})\vec{\mathbf{u}} = (\vec{\mathbf{t}} \otimes \vec{\mathbf{n}})\vec{\mathbf{F}}^{\text{int}}_{ce} \tag{26}$$

The preceding transformation introduces a nonsymmetry in the elemental stiffness matrices of the contact elements. The nonsymmetry is transferred to the global system of equations. With this scheme, the Jacobian matrix of the global system is not symmetric but the convergence of the problem improves substantially.

Taking all contact forces into account, the resultant system for a contact element is

$$[(\vec{\mathbf{n}} \otimes \vec{\mathbf{n}}) + \mu(\vec{\mathbf{t}} \otimes \vec{\mathbf{n}})]\mathbf{K}_{ce}(\vec{\mathbf{n}} \otimes \vec{\mathbf{n}})\vec{\mathbf{u}} = [(\vec{\mathbf{n}} \otimes \vec{\mathbf{n}}) + \mu(\vec{\mathbf{t}} \otimes \vec{\mathbf{n}})]\vec{\mathbf{F}}^{\text{int}}_{ce} \tag{27}$$

Numerically, there is a difference between the normal forces and the frictional forces in contact elements. The stress tensor in the contact elements generates the normal force to the surfaces but not the tangential one. Hence, the influence of tangential forces is not included in the geometrical stiffness matrix. Also, these forces are not taken in account for computing the stress history of the contact interface elements.

Wear and Excavation Strategy

Wear and excavation of a geomaterial can be predicted by computing the material that is damaged and has to be removed. New boundaries are defined with the rest of the volume that remains in the analysis domain. The surface properties of the interacting materials control the wear occurring during the frictional contact.

Contact Model with Wear

Mass loss in a cutting tool and the amount of excavated material that is extracted by the machine is modeled via a wear rate function. When a steady state position in the wear mechanism is reached, wear rate is described by a linear Archard-type equation (Rabinowicz 1995) as

J. Eng. Mech., 2010, 136(4): 455-463

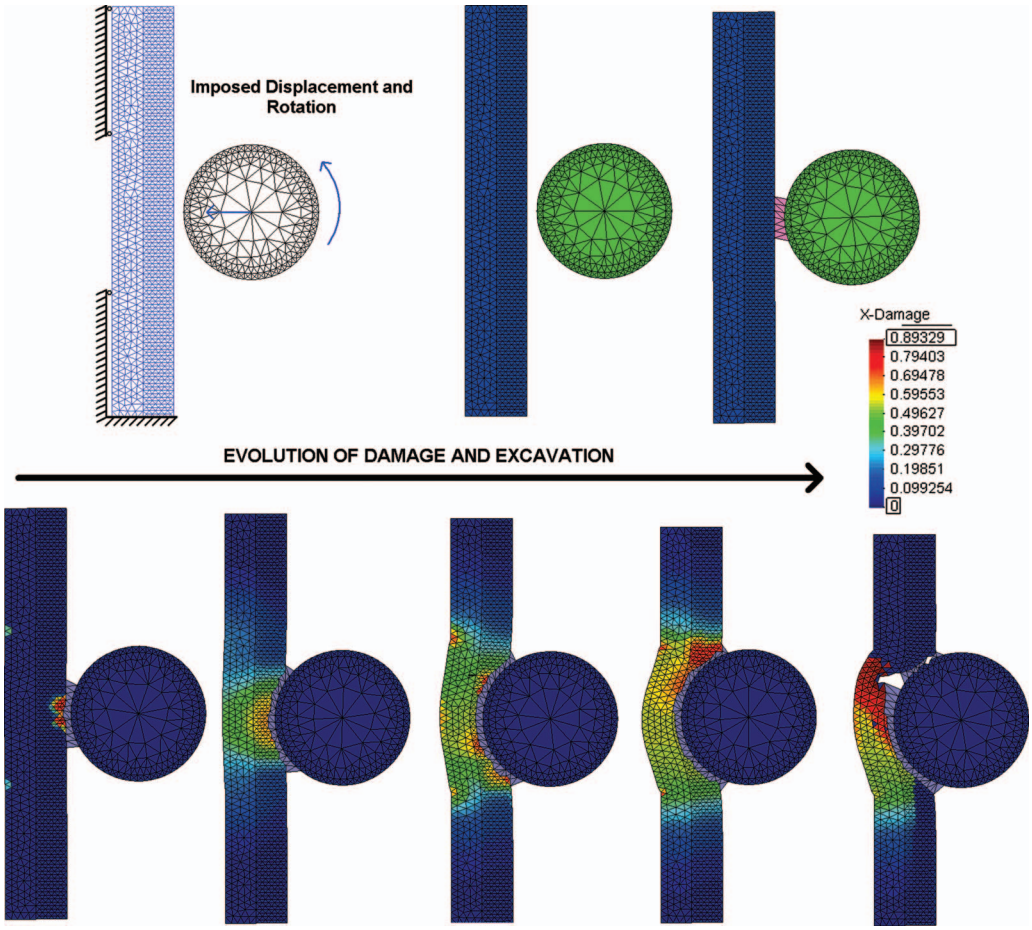

Fig. 5. (Color) Disk excavating a soft wall

$$V_w = K\frac{\|\vec{\mathbf{F}}_n\|}{H}s \tag{28}$$

where $V_w(m^3)$=volume loss of the material along the contact surface; $s(m)$=sliding distance; $\vec{\mathbf{F}}_n(N)$=normal force vector to the contact surface; and $H(N/m^2)$=hardness of the material. Constant K is a nondimensional wear coefficient which depends on the relative contribution of the body under abrasion, adhesion, and wear processes.

In the PFEM, each node on the contact surface has a mesh of elements associated to it. The volume of material wear is compared with the volume associated to each contact node. When both volumes coincide, the node is released and all the elements associated to it are eliminated. The incremental equation for updating the volume of wear at a node is as follows:

$$V_w^{t+\Delta t} = V_w^t + K\frac{\|\vec{\mathbf{F}}_n\|}{H}(\|\dot{\vec{\mathbf{u}}}_t\| \cdot \Delta t) \tag{29}$$

where all variables are nodal variables; $\dot{\mathbf{u}}_t$=relative tangent velocity between the contact surfaces; and Δt=time step.

Geometry Updating

When the volume of worn material associated to a node and the volume of material are the same, the node is released. Elements that contain the released node are eliminated in the next time step. Some particles are also eliminated and hence the global volume of the problem changes. The historical value of the variables in these particles is lost as these particles do not contribute to the system anymore. A scheme of the process is shown in Fig. 4.

The remeshing process allows the boundary recognition and the update of the analysis domain due to the excavation process. The geometry of the analysis domain is changed at each time step as the excavation moves forward.

PFEM Solution Flowchart

The PFEM flowchart for modeling an excavation problem using an implicit time integration scheme is as follows:

1. Read the initial conditions and initialization parameters from a reference mesh:
   a. Nodal variables: $\vec{\mathbf{u}}_0$, $\dot{\vec{\mathbf{u}}}_0$, $\ddot{\vec{\mathbf{u}}}_0$, and $\boldsymbol{\sigma}_0$;
   b. Elemental variables: materials, domains, constitutive laws, . . . ; and
   c. Scalar variables: *time step* (Δt) and *all needed coefficients*;
2. Compute the nodal distance parameters h_{node} for the α shape;
3. Transfer the elemental variables to the nodes (particles);
4. Implicit time integration flowchart $t+\Delta t$:
   a. Estimate a solution $\vec{\mathbf{u}}_\nu$, start Newton iterations $\nu+1$;
   b. Get the elemental variables from their value in the particles;
   c. Compute internal forces $\vec{\mathbf{u}}_\nu$, $\boldsymbol{\sigma}_\nu \rightarrow \vec{\mathbf{f}}^{\text{int}} = \hat{\vec{\mathbf{f}}}^{\text{int}} + \hat{\vec{\mathbf{f}}}^{\text{cont}}$, external forces $\vec{\mathbf{f}}^{\text{ext}}$, and system Jacobian matrix $\mathbf{A} = (\mathbf{M}/\beta\Delta t^2) + \mathbf{K}^{\text{mat}} + \mathbf{K}^{\text{geo}}$;

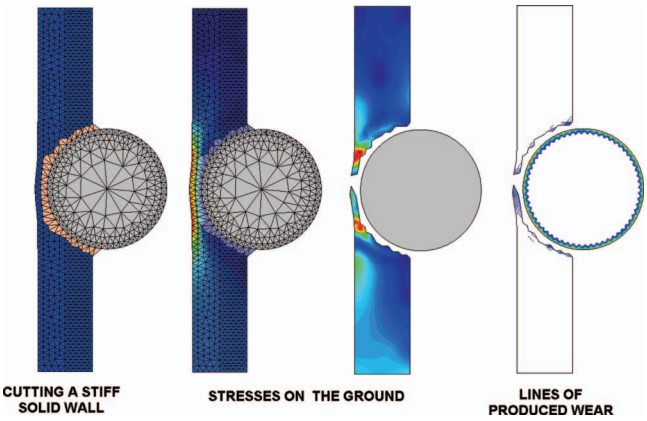

Fig. 6. (Color) Wear and stresses during the excavation of a stiff wall

d. Solve the linear system: $\vec{\mathbf{r}}-\mathbf{A}\Delta\vec{\mathbf{u}}=0$;
e. $\vec{\mathbf{u}}_{\nu+1}=\vec{\mathbf{u}}_{\nu}+\Delta\vec{\mathbf{u}}$; and
f. Check convergence, if not met, go to (a). Compute the variables increment: $\vec{\mathbf{u}}=\vec{\mathbf{u}}_{\nu+1}$, $\Delta\boldsymbol{\sigma}$, $\Delta\boldsymbol{\varepsilon}$ . . . ;

5. Incremental update:
   a. Particle positions: $\vec{\mathbf{x}}^{t+\Delta t}=\vec{\mathbf{x}}^{t}+\vec{\mathbf{u}}$;
   b. Velocities, accelerations: $\dot{\vec{\mathbf{u}}}=\dot{\vec{\mathbf{u}}}_{\nu+1}$, $\ddot{\vec{\mathbf{u}}}=\ddot{\vec{\mathbf{u}}}_{\nu+1}$;
   c. Stresses: $\boldsymbol{\sigma}^{t+\Delta t}_{\text{particle}}=\boldsymbol{\sigma}^{t}_{\text{particle}}+\Delta\boldsymbol{\sigma}_{\text{particle}}$;
   d. Strains: $\boldsymbol{\varepsilon}^{t+\Delta t}_{\text{particle}}=\boldsymbol{\varepsilon}^{t}_{\text{particle}}+\Delta\boldsymbol{\varepsilon}_{\text{particle}}$; and
   e. Update the variables of the constitutive law, the wear and the excavation volumes;
6. Create a new mesh:
   a. Check wear and damage on particles: remove excavated particles;
   b. Transfer the domain particles to the mesher;
   c. Apply the α-shape method in the new mesh: Boundary recognition;
   d. Update the variables dimensions: if the number of particles has changed; and
   e. Identify the domains and the interface mesh for contact;
7. Check active contact elements;
8. Estimate the solution for the next timestep; and
9. Output results. If the simulation is not complete, go to 4.

Examples

Some representative examples are presented to show the capacities of the PFEM for modeling excavation problems. The examples represents cutting and excavating processes in 2D and 3D dimensions.

Disk Cutting of a Ground Section

The first example is an elastic disk in 2D. It is pushed against a solid wall. The disk has an imposed rotation to generate friction when contacting with the solid wall. The material is modeled with a simple damage law.

Fig. 5 shows the 2D model. It can be observed that initially the two bodies are not in contact. When the disk comes near the wall contact is detected. An interface mesh of contact elements is generated and it anticipates the contact area. The contacting forces are transmitted through the contact elements to each domain. This interaction damages the solid wall until it crashes. Contact forces are computed in the axis of the disk to yield force and momentum reactions.

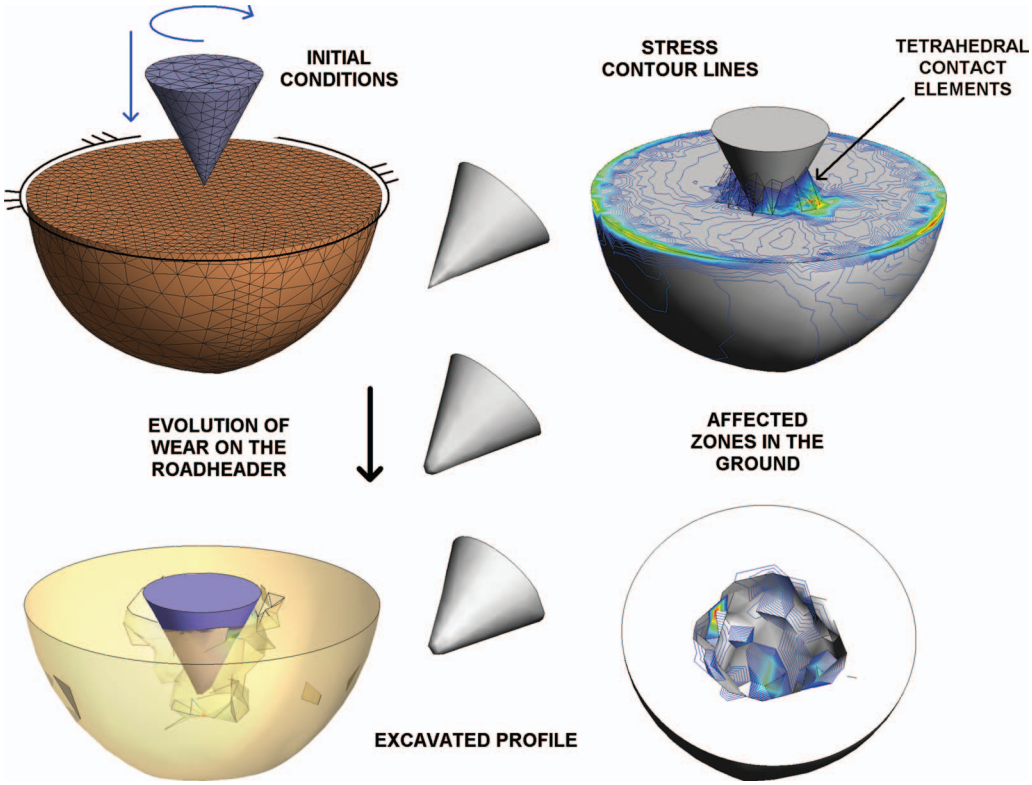

Fig. 7. (Color) Simulation of an excavation with a roadheader

J. Eng. Mech., 2010, 136(4): 455-463

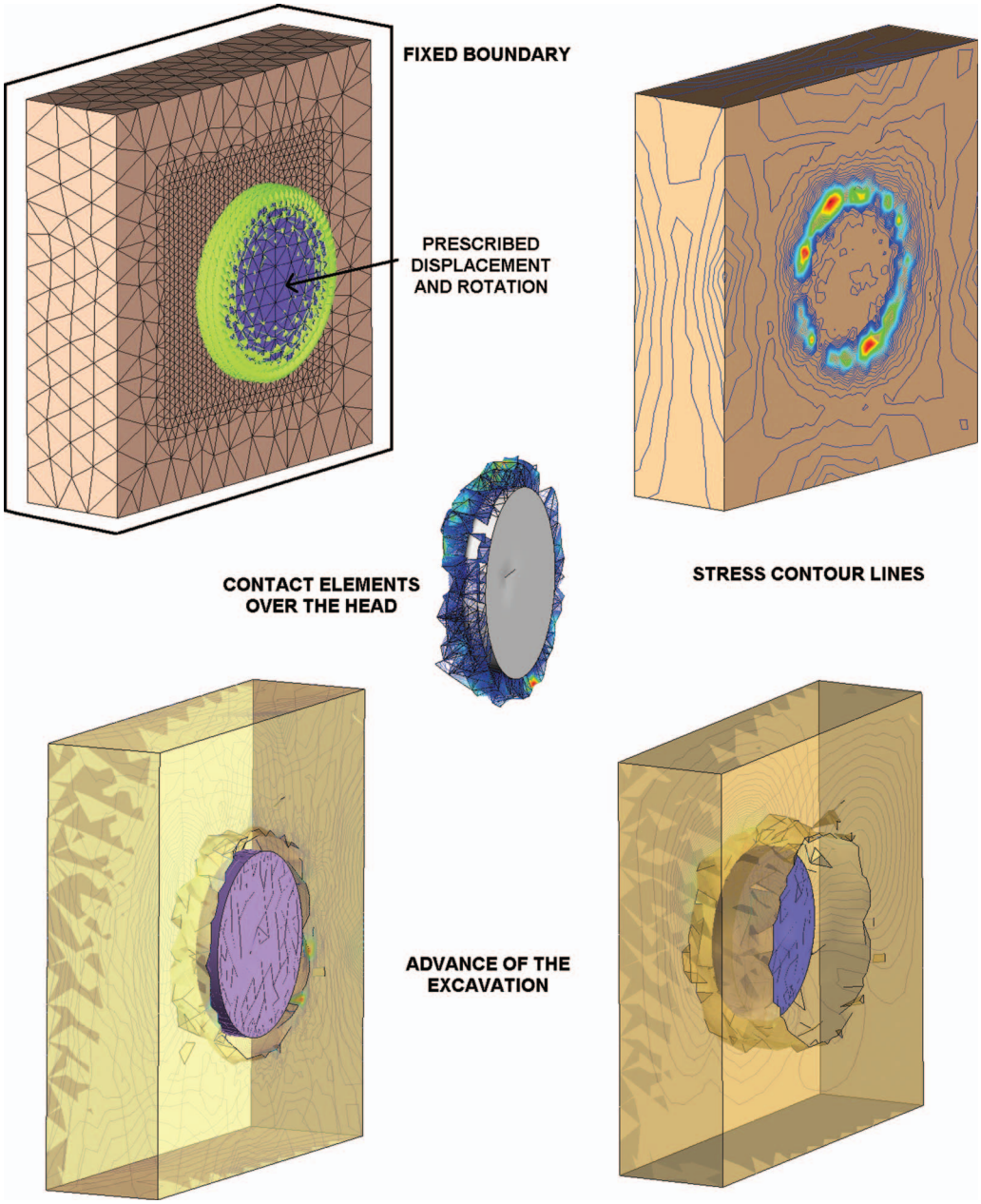

Fig. 8. (Color) Simulation of an excavation with a TBM

The mesh is coarse so as to see the process and the contact interface mesh better. In a fine mesh, contact elements are quite small and are difficult to visualize. It can be seen how as contact forces erode the wall, the excavated particles are taken away from the model. This generates a hollow in the surface while at the same time the material experiences large deformations. In Fig. 6, results of stresses and excavating abrasion for a similar example are presented. In this example the wall material was more rigid but the rest of conditions were the same.

Roadheader Penetrating in the Ground

The next example is a simulation of a roadheader digging a portion of ground. This is an illustrative example of the capabilities of the PFEM for modeling ground excavation and wear of the cutting tools at the same time.

The results are shown in Fig. 7. A rotation and a displacement have been imposed to the roadheader.

Notice that contact elements only appear in the contact zone. The cone that models the roadheader loses material on the tip due to wear. Geometries suffer big changes during the simulation. Remeshing and detection of the boundary via α shape are crucial for capturing the fast changes of the domain boundary.

Simulation of an Excavation with a Tunnel Boring Machine

In Fig. 8, a simulation of a tunnel boring machine (TBM) as it penetrates a 3D domain is presented. This is an example of the capability of the PFEM method to model all type of excavation settings. Fig. 8 shows the stress contour lines on the domain. Far away from the rotating axis, the displacement is bigger for the

same rotation velocity and it generates larger friction forces at the end part of the tunneling head. Fig. 8 also shows the geometry of the interior part of the domain after the excavation. The previous examples are only preliminary results that illustrate the good capabilities of the PFEM for modeling ground excavation processes.

Conclusions

This work presents advances in the numerical modeling of ground excavation using a new method, the PFEM, which is an alternative to the DEM for the simulation of these type of problems. The examples presented show that the PFEM has an excellent performance for the modeling of large problems and global excavation processes.

The major contributions of the work are:

- The development of PFEM in the field of solid mechanics and the adaptation for modeling ground excavation;
- The development of contact mechanics in the PFEM. A new treatment of the contact problem is presented in this work;
- The adaptation of the classical material wear theory to model numerically tool wear and excavation, via coupling FEM with automatic geometry shaping; and
- A global PFEM solution scheme is created by assembling all these single contributions. They set a powerful tool for simulating a wide range of excavation processes, from a full tunneling machine to a single cutting tool.

The remarkable advantages of the PFEM are:

- The method is based on the standard FEM, which permits the use of well-known constitutive equations and all the existing background knowledge in the method. This is an advantage compared with the DEM, which lacks this fundamental base in the constitutive modeling; and
- Preliminary results show that the PFEM is a better alternative than DEM to model excavation problems, due to its greater accuracy and computational efficiency for solving large scale 3D problems of practical interest in civil engineering.

References

Bathe, K. (1982). *Finite element procedures in engineering analysis*, Prentice-Hall, Englewood Cliffs, N.J.

Belytschko, T., Liu, W., and Moran, B. (2000). *Nonlinear finite elements for continua and structures*, Wiley, New York.

Calvo, N., Idelsohn, S., and Oñate, E. (2003). "The extended Delaunay tessellation." *Eng. Comput.*, 20, 583–600.

Edelsbrunner, H., and Mücke, E. (1994). "Three dimensional alpha shapes." *ACM Trans. Graphics*, 13(1), 43–72.

Idelsohn, S., Oñate, E., Calvo, N., and Del Pin, F. (2003). "A Lagrangian meshless finite-element method applied to fluid-structure interaction problems." *Comput. Struct.*, 81, 655–671.

Idelsohn, S., Oñate, E., and Del Pin, F. (2004). "The particle finite-element method a powerful tool to solve incompressible flows with free-surfaces and breaking waves." *Int. J. Numer. Methods Eng.*, 61, 964–989.

Kuhl, D., and Crisfield, M. (1999). "Energy-conserving and decaying algorithms in nonlinear structural dynamics." *Int. J. Numer. Methods Eng.*, 45, 569–599.

Labra, C., Rojek, J., Oñate, E., and Zárate, F. (2008). "Advances in discrete element modeling of underground excavations." *Acta Geotech.*, 3, 317–322.

Oliver, J., Cante, J., Weyler, R., Gonzalez, C., and Hernandez, J. (2007). "Particle finite-element methods in solid mechanics problems." *Computational plasticity*, E. Oñate and R. Owen, eds., Springer, New York.

Oliver, J., Cervera, M., Oller, S., and Lubliner, J. (1990). "Isotropic damage models and smeared crack analysis of concrete." *2nd Int. Conf. on Computer Aided Analysis and Design of Concrete Structures*, Zell am See, Austria.

Oñate, E., Celigueta, M., and Idelsohn, S. (2006). "Modelling bed erosion in free surface flows by de particle finite-element method." *Acta Geotech.*, 1(4), 237–252.

Oñate, E., Idelsohn, S., Celigueta, M., and Rossi, R. (2008). "Advances in the particle finite-element method for the analysis of fluid-multibody interaction and bed erosion in free surface flows." *Comput. Methods Appl. Mech. Eng.*, 197(19–20), 1777–1800.

Oñate, E., Idelsohn, S., Del Pin, F., and Aubry, F. (2004). "The particle finite-element method: An overview." *Int. J. Numer. Methods Eng.*, 1(2), 964–989.

Rabinowicz, E. (1995). *Friction and wear of materials*, Wiley, New York.

Wriggers, P. (2006). *Computational contact mechanics*, 2nd Ed., Springer, New York.